

Novel nickel(II) and manganese(III) complexes with bidentate Schiff-base ligand: synthesis, spectral, thermogravimetry, electrochemical and electrocatalytic properties

Brahim Bouzerafa² · Ali Ourari¹ · Djouhra Aggoun¹ ·
Ramiro Ruiz-Rosas³ · Yasmina Ouennoughi¹ ·
Emilia Morallon⁴

Received: 23 July 2015 / Accepted: 17 October 2015
© Springer Science+Business Media Dordrecht 2015

Abstract An unsymmetrical bidentate Schiff base ligand, ethane 2-(4-methoxyphenyl)-1-iminosalicylidene, and its novel two mononuclear complexes, Nickel(II) [Ni(II)-2L] and Manganese(III) [Mn(III)Cl-2L] where L represents the ligand, have been synthesized and characterized by various physicochemical methods. The Ni(II) ion is coordinated by two nitrogen and two oxygen atoms with both the bidentate Schiff base ligands in an approximately square planar coordination geometry, while the manganese complex, the Mn(III) ion, is involved in an additional contact with one chloride anion for which the coordination sphere appears as a square pyramidal arrangement. The thermogravimetric analyses of the synthesized compounds revealed three different stages of decomposition for NONO bis-bidentate manganese and nickel complexes. The cyclic voltammetry studies of these complexes in *N,N*-dimethylformamide showed a redox couple for each one of them, such as Ni(II)/Ni(I) and Mn(III)/Mn(II), which are quasi-reversible. Their catalytic behaviors were tested showing that the nickel complex is an effective electrocatalyst in the reduction of bromocyclopentane. Regarding the manganese complex, it was revealed that it is an efficient catalyst in the activation of molecular dioxygen,

✉ Brahim Bouzerafa
bouzer.brah@gmail.com

✉ Djouhra Aggoun
aggoun81@yahoo.fr

¹ Laboratoire d'Electrochimie, d'Ingénierie Moléculaire et de Catalyse Redox (LEIMCR), Faculté de Technologie, Université Ferhat ABBAS Sétif-1, 19000 Sétif, Algeria

² Laboratoire de Préparation, Modification des Matériaux Polymériques Multiphasiques (LMPMP), Faculté de Technologie, Université Ferhat ABBAS Sétif-1, 19000 Sétif, Algeria

³ Departamento de Química Inorgánica, Instituto Universitario de Materiales, Universidad de Alicante, Ap. 99, 03080 Alicante, Spain

⁴ Departamento de Química Física, Instituto Universitario de Materiales, Universidad de Alicante, Ap. 99, 03080 Alicante, Spain

currently applied in oxidation reactions of hydrocarbons according to the monooxygenase enzymes as those of cytochrome P450 model.

Keywords Bidentate Schiff base ligand · Nickel and manganese complexes · Cyclic voltammetry · Thermogravimetric analysis · Catalytic behavior

Introduction

Schiff base ligands have been connected with the progress of coordination chemistry since the late nineteenth century. They have played a major role in the development of the coordination chemistry, providing various effects and steric interactions including diverse geometries [1–4]. These complexes may be considered as new class of coordination chemistry compounds when compared to porphyrinic complexes [5].

The methoxy substituent is interesting in the field of Schiff base complexes, [6, 7] since it offers the opportunity to study it as functional group inducing an electron donor effect. Consequently, its position isomers in the monosubstituted aromatic compounds either as primary amines [8] or in the carbonyls compounds [9] have previously been well discussed. The bidentate Schiff base ligands containing the methoxy group have been found to be useful for versatile applications covering a wide range of areas such as catalysis, electrocatalysis, biochemistry, electrochemistry, and spectroscopy [10–13].

In the case of electrocatalysis knowledge, the role played by such structural and electronic effects to control the electrochemical properties of these complexes has been proved to be critical [14]. However, Schiff base complexes are efficient as electrode modifiers for anodic oxidation or cathodic reduction. The anodic oxidation reactions are suitable for electrosynthesis of polymers owing to their high ability to efficiently stabilize the radical-cation, currently involved in most electropolymerization processes useful for the fabrication of modified electrodes [15]. On the other hand, the methoxylated complexes may be considered as catalysts of choice for the electroreduction reactions, seeing that, hypothetically, their ligands are not easily reduced. This is due to an excess of negative charge induced by the methoxy group on the metallic center [16].

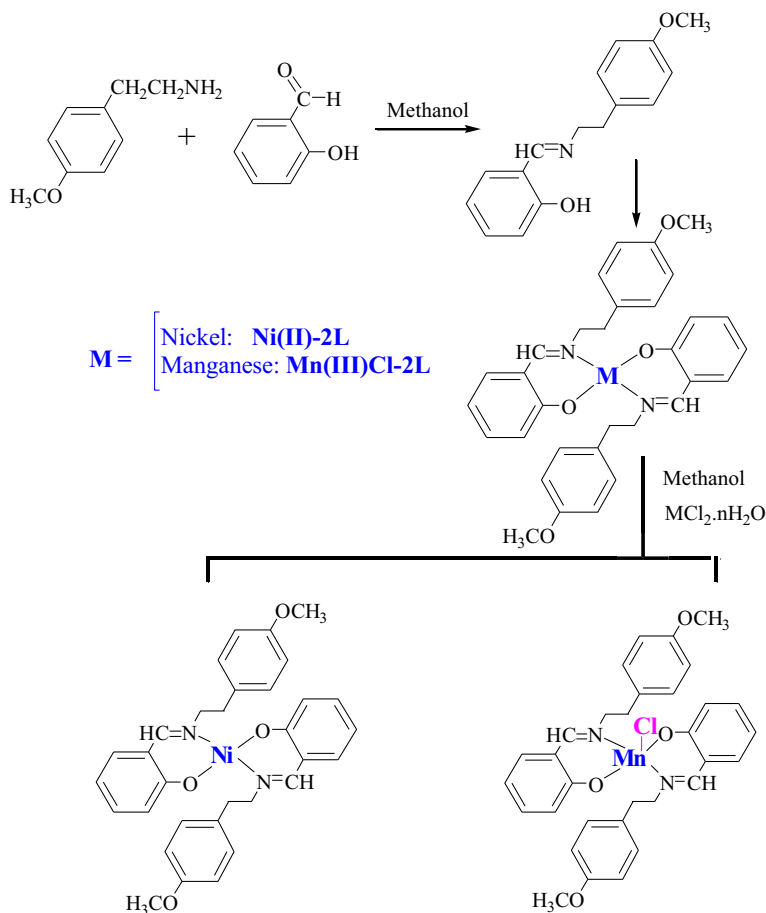
Coordination chemistry offers a wide range of 3d and 4f metals with several oxidation degrees and different geometries associated to the complexes dia- or paramagnetic [17]. Thus, manganese and nickel have received greatest interest for their redox active role in different chemical, electrochemical, biochemical and electrocatalytical processes.

So, manganese has played an important role for its redox active character in catalytic processes particularly with olefins epoxidation [18] or hydrocarbons oxidation [19]. Taking into account their low cost, easy preparation and large availability, the epoxidation of olefins is among the most important reactions in organic chemistry, since it provides an effective way to produce several compounds, among them epoxy resins [20] and chiral compounds, obtained with the use of Jacobsen [21] and catsuki catalysts [22]. Additionally, the complexes containing

Mn(III) centers have excellent magnetic properties because of their high spin of the metallic ion, Mn(III).

As for the nickel redox centers, their complexes showed high catalytic activity towards the oxidation of small organic compounds such as methanol (fuel cells) [23]. For this reason, particular attention has been focused for a long time on nickel complexes used as modifying agents, such as porphyrins and Schiff base. Furthermore, electrogenerated nickel(I) complexes have also been used extensively as catalysts for the reductive cleavage of carbon–halogen bonds in a wide variety of organic compounds [24].

This work is a continuation of our previous studies on the preparation of Schiff base ligands with different electronic and/or steric properties using transition metal complexes **Ni(II)-2L** and **Mn(III)Cl-2L**. The reaction ways leading to the synthesis of the ligand (**HL**) and its corresponding complexes are shown in Scheme 1.



Scheme 1 Proposed synthesis and structures of the Schiff base ligand (**HL**) and the corresponding nickel and manganese complexes

Experimental

Physical measurements

All the chemicals were purchased from commercial sources and used without any further purification. The purity of the synthesized compounds was checked by TLC using glass plates, precoated with silica gel (60F; Merck). ^1H NMR and ^{13}C NMR spectra were recorded on a Bruker 400 MHz spectrometer with CDCl_3 as solvent and tetramethylsilane (TMS) as the internal standard. Chemical shifts are expressed in δ (ppm) units and coupling constants are given in Hertz (Hz). High-resolution mass spectra (HRMS) were acquired by the electrospray ionization (ESI) technique with the aid of a Bruker APEX-2 instrument. FT-IR spectra were recorded as KBr disks on a Perkin-Elmer 1000 FTIR Spectrophotometer while the UV–visible spectra were obtained on a UNICAM UV-300 spectrophotometer with DMF solutions (1 cm, cell).

Thermal analysis (TG and DTG) were obtained in a nitrogen atmosphere using a TGA Perkin Elmer thermal analyzer. The heating rate was set at $10\text{ }^\circ\text{C min}^{-1}$ and the weight loss was measured from ambient temperature up to $950\text{ }^\circ\text{C}$.

Cyclic voltammetry experiments were carried out in an undivided Metrohm cell of 5 cm^3 using a Voltalab 40 (potentiostat/galvanostat) PGZ 301. A planar, circular glassy carbon (GC) electrode (Ø , 3 mm) was employed as the working electrode and a platinum wire as the auxiliary (counter) electrode. All potentials are quoted with respect to the saturated calomel electrode (SCE). An amount of 0.1 M Tetra-*n*-butylammonium tetrafluoroborate (TBABF_4) was used as the supporting electrolyte and DMF as the solvent in all the electrochemical experiments.

Preparation of 2-(4'-methoxyphenyl)-1-iminosalicylideneethane (**HL**)

An amount of 122 mg (1 mmol) of salicylaldehyde was dissolved in 5 mL of methanol. This solution was added drop-wise to 5 mL of methanol containing 151 mg (1 mmol) 4-methoxyphenylethyl amine. The mixture obtained turned rapidly yellow and was then refluxed for 1 h under continuous stirring. The solvent was removed under reduced pressure yielding the expected ligand (**HL**) as suitable crystals. These crystals were recovered by filtration, washed with cold methanol and dried under vacuum (yield 86 %). Selected FT-IR: (KBr, cm^{-1}): ν (3650–3290) (OH); 1630 (C=N); 1240 (C–O); UV–Vis [λ_{max} (nm)]/– ϵ (M cm^{-1}): 314 (14,000).

Preparation of complexes

The metallic chloride salts react with the compound in 2:1 (L:M) molar ratio using a methanolic solution. This synthesis procedure can be employed for the production of both metal chelates with appreciable yields.

Ni(II)-2L complex

An amount of 125.5 mg (1 mmol) of $\text{Ni}(\text{Cl})_2 \cdot 6\text{H}_2\text{O}$ was dissolved in 10 mL of methanol. This solution was added drop-wise to a hot solution of **HL** ligand

containing 512 mg (2 mmol). The mixture rapidly turned green and the reaction was continued with stirring and refluxed for 6 h. The resulting mixture was kept at room temperature for 24 h and the expected compound was recovered by filtration as a green precipitate (yield: 75 %). Microanalysis of $C_{32}H_{32}N_2O_4Ni$ found (calc.) was: C 67.75 % (67.61); H 5.69 % (5.66); N 4.94 % (4.91). Selected FT-IR: (KBr, cm^{-1}) ν : 1610 (C=N); 1246 (C-O); 518 (M-O); 453 (M-N); UV-Vis [$\lambda_{max}(nm)/-\epsilon$ ($M\ cm^{-1}$)]: 314 (18,900); 390 (13,700).

Mn(III)Cl-2L complex

An amount of 198 mg (1 mmol) of $Mn(Cl)_2 \cdot 4H_2O$ was dissolved in 10 mL of methanol. This solution was added drop-wise to a hot solution of **HL** ligand containing 512 mg (2 mmol). The synthesis procedure was kept identical to that described in the previous section (yield: 40 %). Microanalysis of $C_{32}H_{32}N_2O_4MnCl$ found (calc.) was: C 64.16 % (63.78); H 5.38 % (5.29); N 4.68 % (4.65). Selected FT-IR: (KBr, cm^{-1}) ν : 1622 (C=N); 1237(C-O); 568 (M-O); 455 (M-N); UV-Vis [$\lambda_{max}(nm)/-\epsilon$ ($M\ cm^{-1}$)]: 321 (13,700), 375 (64,700).

Results and discussion

We report here on two new nickel(II) and manganese(III) complexes using bidentate Schiff base ligand (**HL**), derived from salicylaldehyde and methoxyphenylethylamine. The electrochemical properties of these two complexes were studied by cyclic voltammetry. In addition, the catalytic performances of these complexes were examined in the electroreduction of dioxygen and bromocyclopentane under diverse experimental conditions. The thermal decomposition and relationship between structure of ligand and their metal complexes were also discussed.

The stoichiometric mixture obtained from salicylaldehyde and 4-methoxyphenyl ethylamine in methanol solution gave the desired bidentate ligand (**HL**) [25]. This ligand is soluble in all common organic solvents like alcohols, dimethylformamide (DMF), dimethylsulfoxide (DMSO) and acetonitrile. The elemental analysis along with the FT-IR and UV-Vis measurements demonstrate that all the obtained complexes have (1:2) metal-ligand stoichiometry and show a composition in good agreement with the proposed formulae. The chelates were proven to be stable under the atmospheric conditions either when stored in solution or as pure solids.

Spectroscopic properties

UV-Visible spectroscopy

Figure 1 shows the UV-Vis spectra of the ligand and their metal complexes. The electronic spectra of the ligand (**HL**) and the two complexes were recorded in DMF solutions (10^{-5} M) at room temperature. In the UV-Vis spectra of the parent ligand, an intense absorption band at around 314 nm was assigned to the $n \rightarrow \pi^*$ of azomethine groups. This band is present in the electronic absorption spectra of the

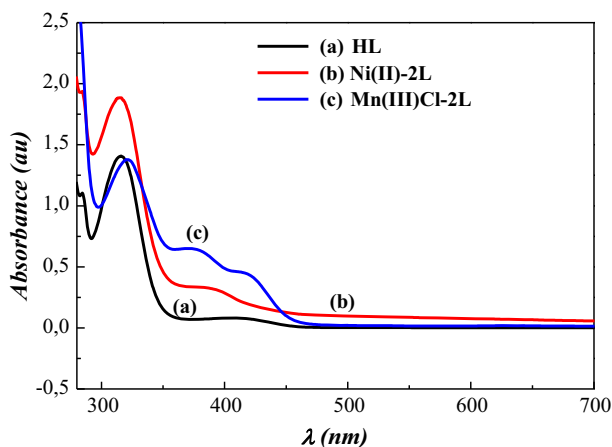


Fig. 1 UV-Vis spectra of ligand (HL) and its metal complexes Ni(II)-2L and Mn(III)Cl-2L

complexes showing no significant shift for the nickel complex and only a reduced shift (7 nm) in the case of the manganese one. The electronic spectra of the two complexes also give information about metal–ligand binding in the complexes. Their electronic absorption spectra showed a peak between 350 and 400 nm which could be assigned to the charge transfer band, while the weak band observed at about 420 nm for the manganese complex is assignable to the MLCT, demonstrating the coordination of the metallic center to the ligand with coordinating bonds between the (Ph-O) phenoxy and the (C=N) azomethine functions [26].

FT-IR spectroscopy

Figure 2 presents the FT-IR spectra of the ligand and the metal complexes. The infrared spectra are consistent with the formation of the Schiff base ligand. The IR spectrum of the free ligand exhibits a broad absorption band in the range of $3650\text{--}3290\text{ cm}^{-1}$ centered at 3442 cm^{-1} , characteristic of the stretching vibration of the OH phenolic groups fixed on the phenyl ring. A second set of characteristic bands observed around 3010 cm^{-1} can be related to the presence of aromatic ν (C–H). The fundamental stretching mode of azomethine ν (C=N) can be readily assigned by comparison between the infrared spectrum of the reagents, salicylaldehyde and 2-(4-methoxyphenyl)ethanamine, and the resulting product [27]. The absorption bands of the --NH_2 function in 2-(4-methoxyphenyl)ethanamine and the ν (C=O) carbonyl function of the salicylaldehyde disappear to the benefit of the ν (C=N) azomethine group, confirming that the condensation reaction has occurred. The most intense absorption band, observed at 1630 cm^{-1} , is assigned to the --C=N-- stretching frequency of the azomethine moiety of the bidentate ligand. Finally, the band located at 1240 cm^{-1} is attributed to the ν (=C–O) phenolic groups [28].

In the case of the complexes, the strong absorption band corresponding to the ν (C=N) group is shifted to the lower frequencies by $20\text{--}30\text{ cm}^{-1}$, indicating the involvement of the nitrogen atom of the ν (C=N) imine function in the coordination

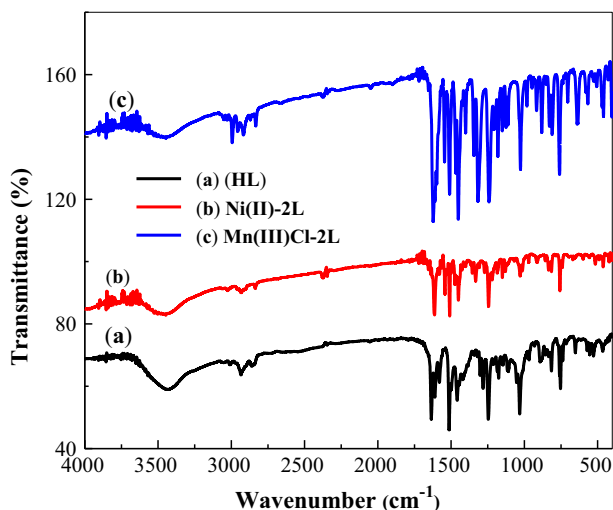


Fig. 2 FT-IR spectra of ligand (**HL**) and its metal complexes **Ni(II)-2L** and **Mn(III)Cl-2L**

of the metal ion (Fig. 2). In the reverse case, the ν ($=C-O$) absorption bands are instead shifted to the higher frequencies around $1310\text{--}1340\text{ cm}^{-1}$ [29] by a strengthening of electronic density provided from the metal ion. Furthermore, in coordination chemistry, the complexes exhibit the formation of metal–nitrogen bonds. This is further supported by the appearance of an absorption band corresponding to the metal nitrogen ν ($M-N$) stretching vibration at around $440\text{--}470\text{ cm}^{-1}$ [30]. Further conclusive evidence for the formation of metal–oxygen bonds is the appearance of new bands around $540\text{--}570\text{ cm}^{-1}$, which are attributable to the metal–oxygen bonds stretching vibrations [31].

¹H and ¹³C NMR spectroscopy

The ^1H NMR spectrum of the ligand (**HL**) in CDCl_3 is shown in Fig. 3 in which the phenolic proton of the salicylidene moieties may be observed at chemical shifts more than 10 ppm. The ^1H NMR spectra of the ligand have shown a sharp singlet signal at 7.240 ppm due to the azomethine protons. Other signals which have appeared as multiplets (m) in the aromatic region at around 5.861–6.348 ppm are assignable to the aromatic protons. The (OCH_3) methoxy protons absorb at 2.813 ppm with the expected signal integration. The $\text{CH}_2\text{-NH}_2$ protons of the ethylene group are also observed as a triplet at 1.983 ppm. Regarding the CH_2 -phenyl, it resonates at weak fields due to the presence of an adjacent aromatic ring inducing a significant deshielding effect on the chemical shift value obtained at 2.840 ppm.

The ^{13}C NMR spectrum of the ligand (**HL**) was also recorded in CDCl_3 and is presented in Fig. 4. The results obtained for this compound are consistent with those reported in the literature [32] describing similar structures. The carbon of the methoxy group is responsible of the peak observed at 55.43 ppm while the

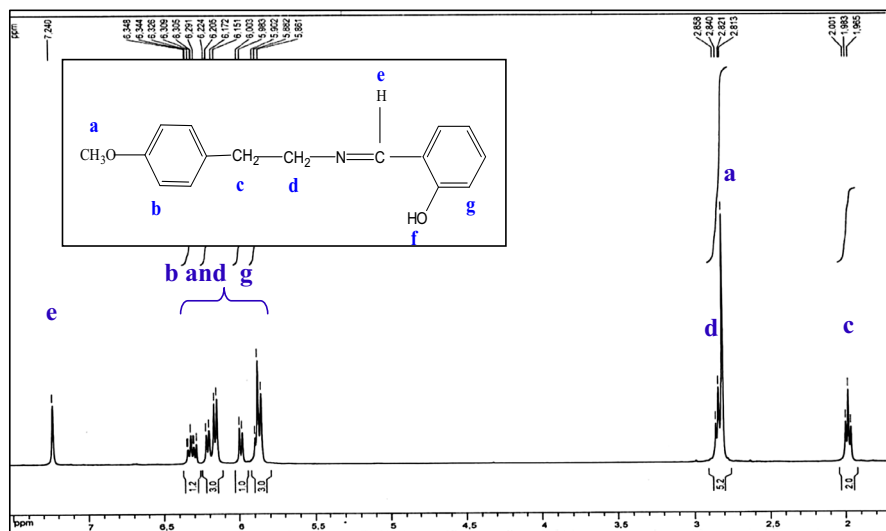


Fig. 3 ^1H NMR spectrum of the ligand (HL)

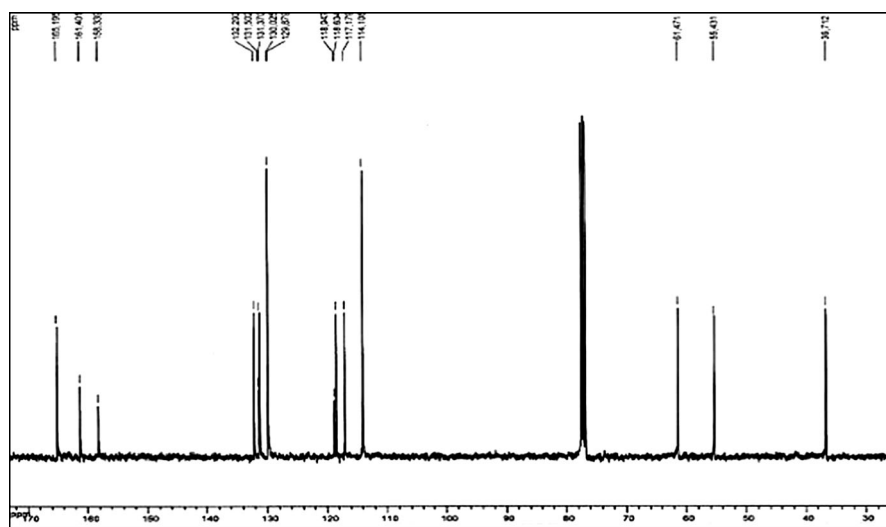


Fig. 4 ^{13}C NMR spectrum of the ligand (HL)

azomethinic carbon is located at 165.339 ppm [33]. The signals observed at 161.40 and 158.33 ppm are assigned, respectively, to the phenolic (C–OH) and phenoxy (C–O–C) groups [34]. Also, the spectrum showed peaks at 132–114 ppm corresponding to carbons of the phenyl ring. As for the $\text{CH}_2\text{--NH}_2$, it resonates at 36.71 ppm whereas the $\text{CH}_2\text{--phenyl}$ is shifted to the weaker fields and observed at 61.47 ppm. These signals are fully compatible with the number of their carbon atoms.

Mass spectrometry

The electronic impact mass spectra of the bidentate Schiff base (Fig. 5a) show the mainly intense molecular ion peak at $m/z = 256.2$, which corresponds to the expected molecular weight of the ligand. The **Ni(II)-2L** complex (Fig. 5b) and the **Mn(III)Cl-2L** complex (Fig. 5c) also share the same fragmentation pathway. In addition, the high resolution mass spectra (HRMS) show multiple peaks that come from the different fragments of the parent molecule, as well as an ion peak observed at $m/z = 135.1$, which is also found in the spectrum of the ligand. As can be seen in Scheme 2, the diverse fragments observed are in good agreement with the proposed molecular structure of the ligand. Thus, it was also confirmed that the studied complexes were formerly constituted by two ligand units adopting a mononuclear behavior when recording their HRMS mass spectra. These observations were found to be in perfect agreement with the formula suggested early from the elemental analysis.

Thermogravimetric analyses

Thermal behavior of the ligand and its metal complexes has been performed in temperatures ranging from 25 to 950 °C under nitrogen atmosphere at a heating rate of 10 °C.min⁻¹. The thermogravimetric (TG-DTG) analyses of ligand (**HL**) and both its metal complexes, **Ni(II)-2L** and **Mn(III)Cl-2L**, are illustrated in Fig. 6. The main results are summarized in Table 1.

Two well-differenced mass loss steps are clearly observed showing the pathway decomposition. The components involved in these decomposition processes relate to the ligand structure, generating unstable intermediates that evolve as gaseous products. In the case of the (**HL**) (Fig. 6a) ligand, the first weight loss step starts from 285 up to 457 °C corresponding to the removal of the C₁₆H₁₆ON molecular residue with weight loss estimated at 92.44 % (calculated 93.33 %). In the last part of the thermogram covering the range 457–800 °C, the observed weight loss is evaluated to 7.56 % (calculated 6.65 %) corresponding to the loss of the hydroxyl group (OH).

For the nickel complex, the TG analysis (Fig. 6b) revealed that its decomposition is produced in three steps. The first is accompanied by a weight loss of 2.72 % (calculated 2.64 %) which is ascribed to the loss of the methyl (–CH₃) group within the temperature range 171–259 °C. The second step shows a weight loss within the temperature range of 259–334 °C. This is due to the elimination of coordinated oxygen atoms, with a weight loss of 3.12 % (calculated 2.82 %). The last step starts from 334 and ends at 485 °C ($T_{\max} = 375.6$ °C) and is attributed to the decomposition of the coordinated molecular form C₂₅H₂₃N₂O with a weight loss of 65.30 % (calculated 64.77 %).

The Schiff base manganese complex **Mn(III)Cl-2L** also decomposes via three steps. This decomposition starts from 225 and ends at 765 °C (Fig. 6c). The first decomposition step produces an observed weight loss of 35.68 % (calculated 36.04 %) that has been assigned to the loss of two C₁₀H₁₁NO moieties with the HCl molecule [35]. The second step occurs at temperatures ranging from 360 to 495 °C,

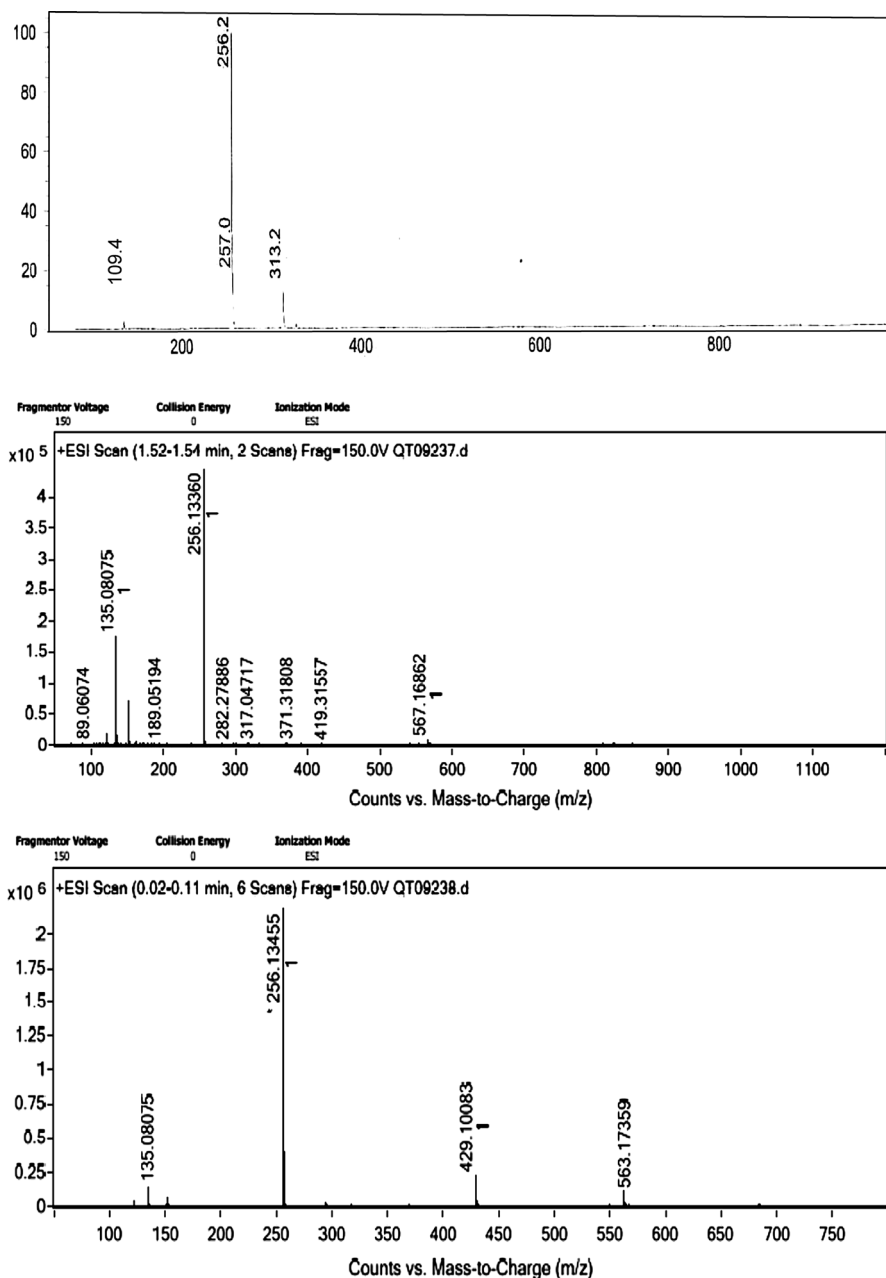
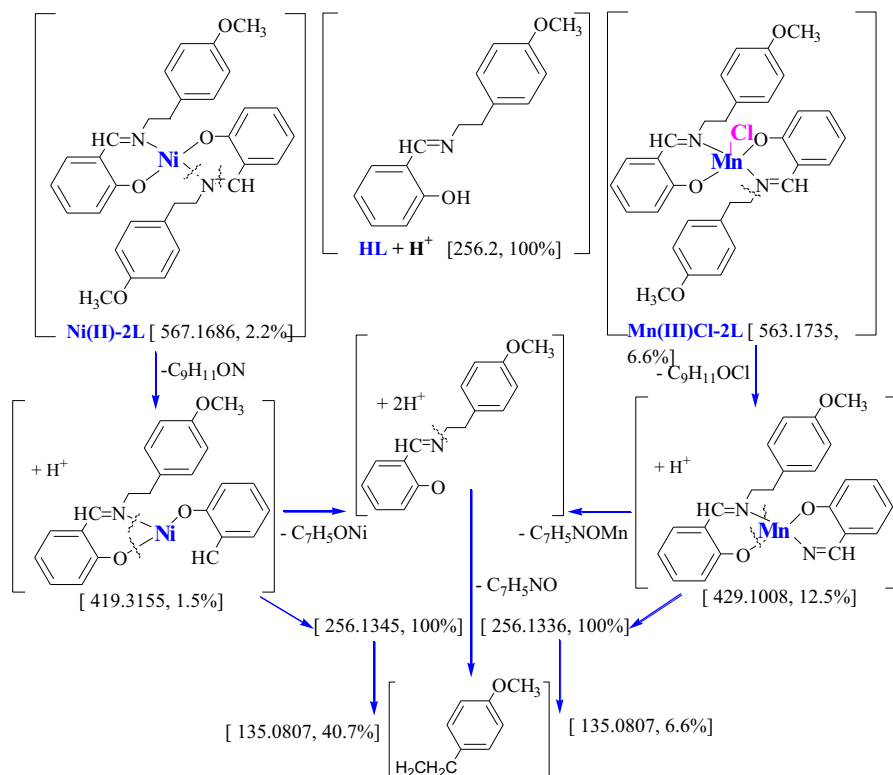


Fig. 5 Mass spectra of **HL**, **Ni(II)-2L** and **Mn(III)Cl-2L**

and has been attributed to the removal of the phenylene group (C_6H_4), corresponding to a weight loss of 8.21 % (calculated 7.61 %). The last step probably represents the loss of the last C_6H_4 phenylene group as mentioned above



Scheme 2 The fragments observed in the mass spectra of **HL**, **Ni(II)-2L** and **Mn(III)Cl-2L**

with a weight loss of 8.14 % (calculated 7.61 %). The results obtained from thermogravimetric analyses are given in Table 1. Therefore, it has been found that the decomposition pathway of the **Mn(III)Cl-2L** corroborates the suggested decomposition process illustrated in Scheme 1.

Electrochemistry

Electrochemical behavior of the ligand HL

The electrochemical response of the ligand was studied by cyclic voltammetry using a scan rate of 100 mV s^{-1} , exploring potentials from -2.0 V to $+2.0 \text{ V}$ (Fig. 7). The voltammogram shows two oxidation waves, at $E_{p_{a1}} = 0.232$ and $E_{p_{a2}} = 1.374 \text{ V}$, versus SCE, respectively. The first oxidation wave is probably assignable to the oxidation of methoxy substituents as reported in the literature [36]. As has been proposed, the oxidation wave corresponds to the formation of radical-cations as the first step. This intermediate is not stable due to its high chemical reactivity [37]. The second may be assigned to the oxidation of the phenolic function. These results may approach those reported in the literature [38] for the

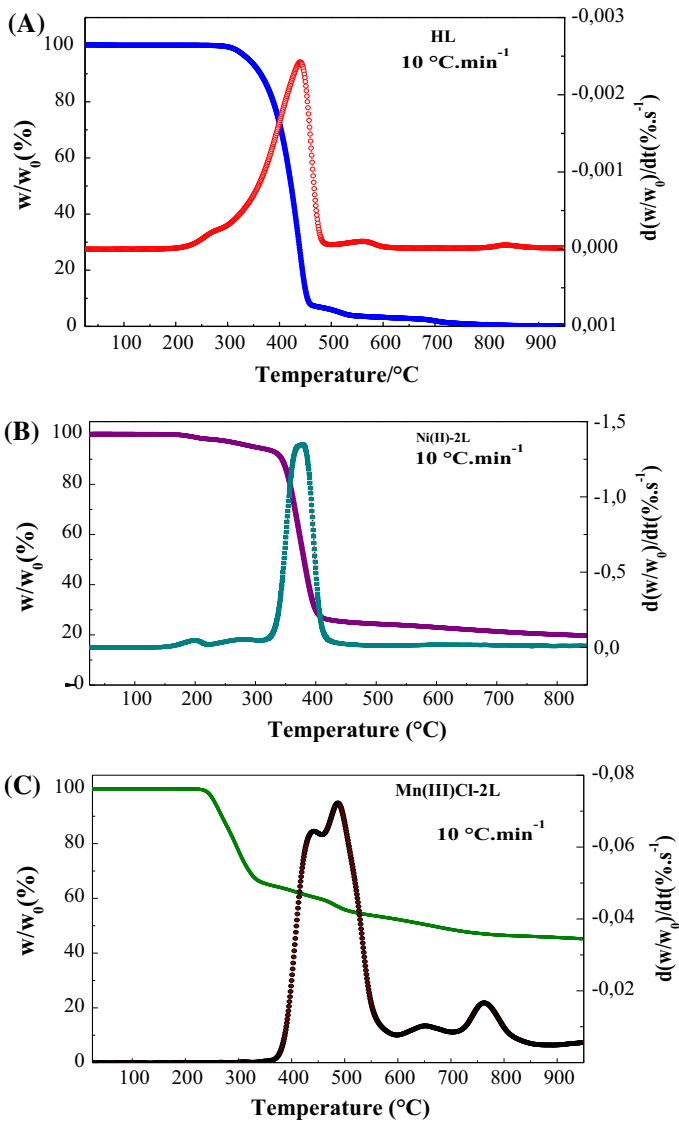
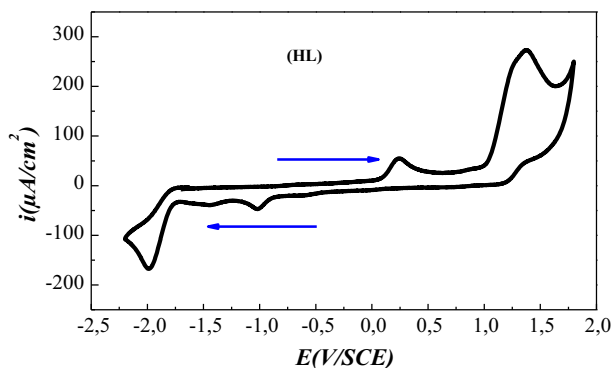


Fig. 6 a TG-DTG curves of **HL**, **b Ni(II)-2L** and **c Mn(III)Cl-2L**

compounds showing a similar structure. Concerning the reduction sweep, three reduction waves are observed at $E_{pc1} = -1.010$, $E_{pc2} = -1.450$ and $E_{pc3} = -1.976$ V/SCE, respectively. The first is attributed to the reduction of the oxidized function indicated earlier, while the second may most probably be due to the reduction of the $-C=N-$ (azomethine) group of the adsorbed molecule [39]. As for the last wave, it seems to be an irreversible system and may be ascribed to the reduction of the imino function.

Table 1 Thermogravimetric results of ligand (HL) and its metal complexes Ni(II)-2L and Mn(III)Cl-2L

Compound	Number of steps	Temp. range (°C)	DTG T_{max} /°C	Mass loss (%) found (calcd.)	Product	Residue
HL	Step 1	285–457	440.6	92.44 % (93.33 %)	Loss of $C_{16}H_{16}ON$	
	Step 2	457–800	561.1	7.56 % (6.65 %)	Loss of OH	
Ni(II)-2L	Step 1	160–259	196.7	2.72 % (2.64 %)	Loss of CH_3	$NiO_2 + C_6H_6$
	Step 2	259–334	269.4	3.12 % (2.82 %)	Loss of O	
	Step 3	334–485	375.6	65.30 % (64.77 %)	Loss of $C_{25}H_{23}N_2O$	
Mn(III)Cl-2L	Step 1	225–360	486.5	34.73 % (35.76 %)	Loss of $C_{20}H_{24}O_2N_2Cl$	MnO_2
	Step 2	360–495	645.4	8.21 % (7.61 %)	Loss of C_6H_4	
	Step 3	495–755	761.5	8.14 % (7.61 %)	Loss of C_6H_4	

**Fig. 7** Cyclic voltammogram of 1 mM HL on GC electrode in DMF solution, 0.1 M TBAPF₄ at 100 mV s⁻¹ from -2.2 to 2.2 V versus SCE

Electrochemical behavior of the nickel complex Ni(II)-2L

Figure 8 illustrates the voltammetric behaviour of the Ni(II)-2L complex, recorded on the GC-electrode in DMF solutions at 100 mV/s as scan rate. Its cyclic voltammetric curves for the anodic oxidation show two redox couples at $E_{1/2} = +0.745$ and $E_{1/2} = +1.15$ V/SCE. A single electron is involved in the first oxidation wave which can be assigned to the oxidation of Ni(II) to Ni(III). The second one is due to the oxidation of the Schiff base ligand. As for the return sweep, only one well-defined wave was observed. This wave expresses the monoelectronic transfer leading to the formation of the initial form of the nickel complex according to the redox couple Ni(III)/Ni(II). Its half-wave potential value ($E_{1/2}$) was calculated and found to be equal to -1.48 V/SCE. The electrochemical reduction peak observed at -1.980 V/SCE is due to the irreversible reduction of the ligand [40] (Fig. 8a).

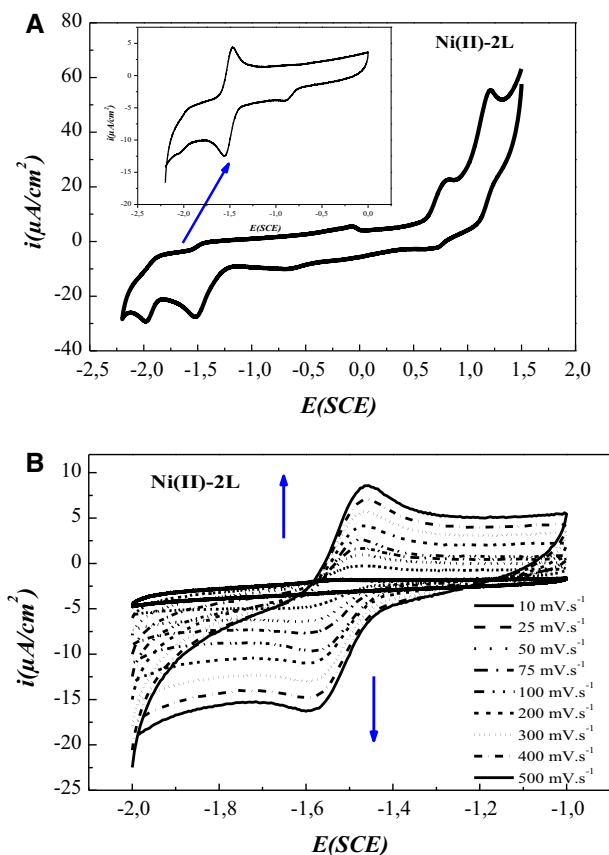


Fig. 8 **a** Cyclic voltammogram of 1 mM Ni(II)-2L on the GC electrode in DMF solution, 0.1 M TBABF₄ at 100 mV s⁻¹. **b** Cyclic voltammogram of 1 mM Ni(II)-2L on the GC electrode in DMF solution with cycling from -1.1 to -1.8 V versus SCE, 0.1 M TBABF₄ at various scan rates

The cyclic voltammogram, recorded in the range between 0.0 and -2.2 V, shows a well-defined redox peak at $E_{pc} = -1.560$ V (cathodic peak) and $E_{pa} = -1.460$ V (anodic peak) which corresponds to Ni(II)/Ni(I) system. We have followed the evolution of the potentials of the anodic and cathodic peak currents depending on the variation of the scan rates for the system.

Ni(II)/Ni(I) between -1.0 and -2.0 V versus SCE (Fig. 8b). In this case, we notice that, after discounting the double layer contribution, the intensity of the peak currents i_{pa} , i_{pc} follows a square-root relationship with the scan rate. It is noticeable that their ratios are close to 1, confirming the occurrence of a reversible process, while the peak-to-peak separation (ΔE_p) was found to be 100 mV and to increase slightly with the scan rate. In spite of a ΔE_p value, corresponding to a quasi-reversible behavior, of the couple Ni(II)L + e⁻ = Ni(I)L which is in agreement with a diffusion-controlled electrochemical process [41]). This ΔE_p value is larger than the theoretical equal to 59.2/n mV (where n is the number of transferred

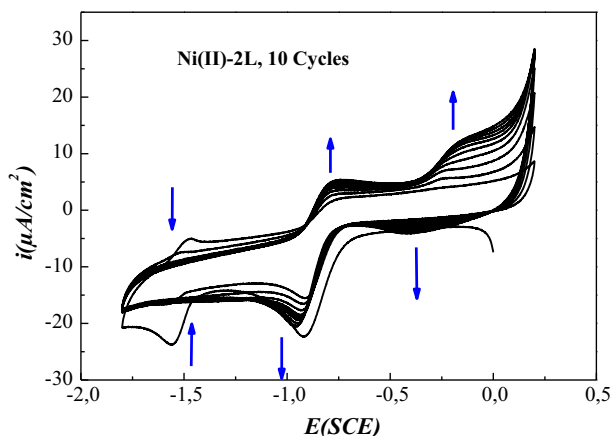


Fig. 9 Cyclic voltammogram showing electrodeposition of poly-[Ni(II)-2L] on the glassy carbon electrode in DMF solution, 0.1 M TBAPF₄ at 100 mV s⁻¹

electrons in the process). This value suggests that the oxidation of nickel (II) in the considered complex should only correspond to one electron charge transfer.

Figure 9 shows the evolution of the cyclic voltammograms of the Ni(II)-2L complex in DMF solutions. The cathodic reduction was achieved by repetitive cycles of the potential at the surface of the glassy carbon electrode between 0.2 and -1.8 V using a scan rate of 100 mV s⁻¹. The build-up of the electropolymerized poly-[Ni(II)-2L] can be followed by an increase of the peaks associated to the redox processes previously discussed. Thus, it is clear that, upon continuous cycles, an electroactive polymer is deposited on the electrode surface. By adjusting the number of CV cycles, different and controllable polymer thicknesses can be obtained [42].

Electrochemical behavior of the manganese complex Mn(III)Cl-2L

Figure 10 depicts the voltammograms (CVs) of the manganese complex which were recorded in the same electrolyte already used for the nickel complex. The CV revealed three new redox systems, different to those detected for the ligand, and appearing at $E_{1/2}(\text{I}) = -0.106$ V, $E_{1/2}(\text{II}) = 0.497$ V and $E_{1/2}(\text{III}) = 0.897$ V (vs. SCE). The $\Delta E_p = (E_{pa} - E_{pc})$ values were estimated to be 100, 110 and 128 mV, respectively, pointing out again the quasi-reversible nature and the participation of only one electron in these redox processes. The first and the second systems are, respectively, attributed to the Mn(II)/Mn(III), Mn(III)/Mn(IV) couples. These redox systems, when analyzed separately on CVs, and recorded with various scan rates from 10 to 500 mV s⁻¹, are illustrated in Fig. 11.

These voltammetric curves seem to maintain the features of a quasi-reversible behavior process, typical for the one electron transfer process commonly known to be diffusion controlled.

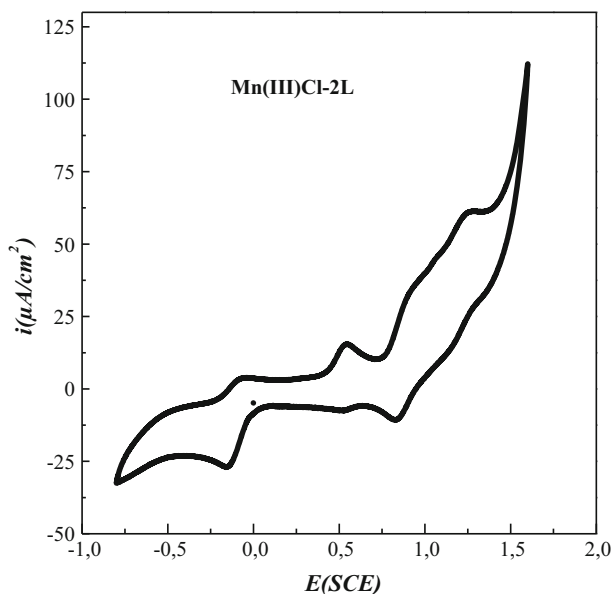


Fig. 10 Cyclic voltammogram of 1 mM **Mn(III)Cl-2L** on the GC electrode in DMF solution, 0.1 M TBABF₄ at 100 mV s⁻¹

Electrocatalytic properties

The electrochemical reduction of bromocyclopentane (BrCP) by the **Ni(II)-2L** complex was used as a catalytic test in order to check the possible electrocatalytic activity of both the complexes synthesized in this work. Figure 12 presents the CV curves, recorded at 100 mV s⁻¹ on the GC-electrode in DMF solutions containing 1.0 mM of the **Ni(II)-2L** complex with 0.1 M of TBABF₄ as supporting electrolyte. In each one of them, different amounts of BrCP were added prior tp starting the CV measurement. When 1 mM of BrCP was added to the solution, a reduction current at -1.45 V versus SCE can be seen in Fig. 12. This reduction peak current (i_{pc}), arising from the addition of the bromocyclopentane molecules is due to the electrocatalytic reduction by the nickel complex used as catalyst. Moreover, the peak potential for the reduction of Ni(II) to Ni(I) is shifted downwards by ca. 15 mV, owing to the rapid reaction between the electrogenerated nickel(I) and bromocyclopentane, while no shifting was observed for the oxidation wave of nickel(I) [43]. The intensity of the reduction peak seems to be proportional to the concentration of BrCP, since the i_{pc} is gradually increased as the concentration of substrate increases. All these features are characteristic of a catalytic reaction in which the Ni complex species act as electrochemical mediators (or catalysts).

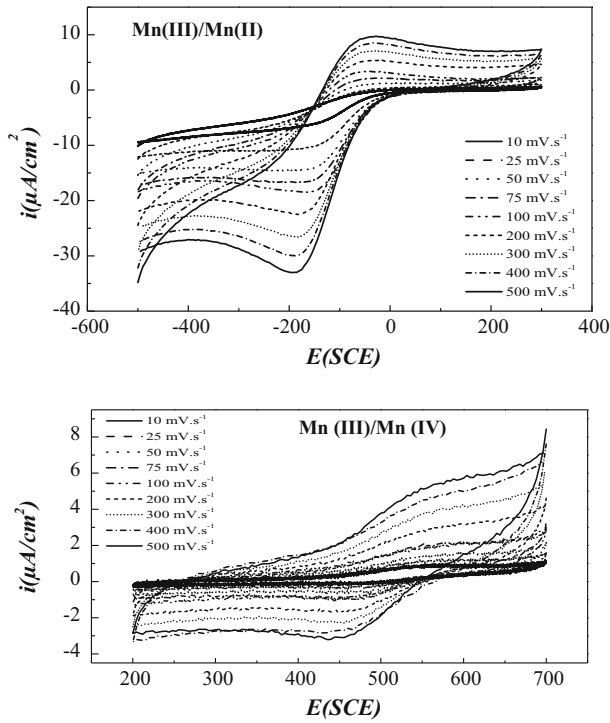


Fig. 11 Cyclic voltammogram of 1 mM Mn(III)Cl-2L on the GC electrode in DMF solution, 0.1 M, TBABF₄ at various scan rates

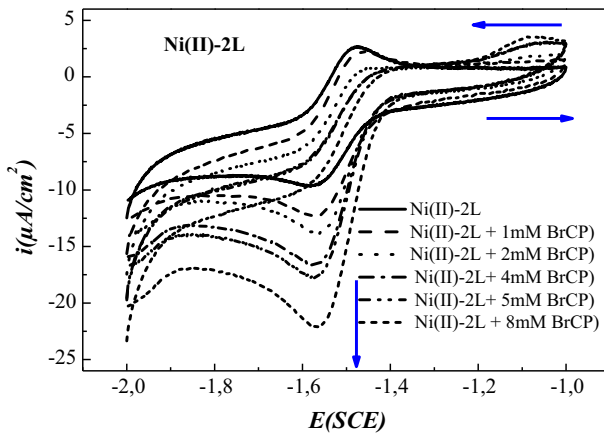


Fig. 12 Cyclic voltammograms recorded on the glassy carbon electrode in DMF solution containing 0.10 M TBAPF₄ and 1.0 mM Ni(II)-2L at 100 mV s⁻¹ without and with different concentrations of bromocyclopentane (BrCP)

Conclusion

In this paper, we have presented the synthesis and characterization of a bidentate Schiff base ligand with its two new metal complexes, **Ni(II)-2L** and **Mn(III)Cl-2L**. This study describes the synthetic methods of a new Schiff base chelate, which includes a methoxy functional group, and its complexes with bivalent and trivalent transition metals such as nickel(II) and manganese(III). These materials have been fully characterized in terms of structure, chemical composition and electrochemical behavior. The nickel complex was easily electropolymerized to its poly-[**Ni(II)-2L**] films yielding modified electrodes. This new complex was also found to be as efficient homogeneous electrocatalyst for the reduction of bromocyclopentane. We also believe that this work will shed light on future work on the synthesis of mono- or multinuclear Schiff base–metal complexes and heterocyclic compounds from Schiff base ligands with methoxy functional groups.

References

1. H. Wang, D. Zhang, Y. Chen, Z. Hai, L. Tian, J. Jiang, Synthesis, crystal structures, and magnetic properties of new tetranuclear Cu(II) complexes of bis-bidentate Schiff-base ligands. *Inorg. Chim. Acta* **362**, 4972–4976 (2009)
2. M. Khorshidifard, H.A. Rudbari, Z.K. Delikani, V. Mirkhani, R. Azadbakht, Synthesis, characterization and X-ray crystal structures of Vanadium(IV), Cobalt(III), Copper(II) and Zinc(II) complexes derived from an asymmetric bidentate Schiff-base ligand at ambient temperature. *J. Mol. Struct.* **1081**, 494–505 (2015)
3. M.T.H. Tarafder, K.T. Jin, K.A. Crouse, A.M. Ali, B.M. Yamin, H.-K. Fun, Coordination chemistry and bioactivity of Ni²⁺, Cu²⁺, Cd²⁺ and Zn²⁺ complexes containing bidentate Schiff bases derived from Sbenzylthiocarbazate and the X-ray crystal structure of bis[S-benzyl-N-(5-methyl-2-furylmethylene)dithiocarbazato]cadmium(II). *Polyhedron* **21**, 2547–2554 (2002)
4. M. Amirnasr, A.H. Mahmoudkhani, A. Gorji, S. Dehghanpour, H.R. Bijanzadeh, Cobalt(II), nickel(II), and zinc(II) complexes with bidentate *N,N'*-bis(b-phenylcinnam aldehyde)-1,2-diiminoethane Schiff base: synthesis and structures. *Polyhedron* **21**, 2733–2742 (2002)
5. A. Deronzier, J.-C. Moutet, Polypyrrole films containing metal complexes: syntheses and applications. *Coordin. Chem. Rev.* **147**, 339–371 (1996)
6. S. Saha, R.K. Kottalanka, P. Bhowmik, S. Jana, K. Harms, T.K. Panda, S. Chattopadhyay, H.P. Nayek, Synthesis and characterization of a nickel(II) complex of 9-methoxy-2,3-dihydro-1,4-benzoxepine derived from a Schiff base ligand and its ligand substitution reaction. *J. Mol. Struct.* **2014**, 26–31 (1061)
7. W.I. Azeez, A.I. Abdulla, Dioxouranium(VI) thiocyanate complexes of schiff bases of p-Nitro, chloro, bromo, hydroxy and methoxy aniline and salicylaldehyde. *Inorg. Chim. Acta* **110**, 15–18 (1985)
8. A.A. Soliman, W. Linert, Investigations on new transition metal chelates of the 3-methoxy-salicylidene-2-aminothiophenol Schiff base. *Thermochim. Acta* **338**, 67–75 (1999)
9. C. Maxim, T.D. Pasatoiu, V.Ch. Kravtsov, S. Shova, Ch.A. Muryn, R.E.P. Winpenny, F. Tuna, M. Andruh, Copper(II) and zinc(II) complexes with Schiff-base ligands derived from salicylaldehyde and 3-methoxysalicylaldehyde: synthesis, crystal structures, magnetic and luminescence properties. *Inorg. Chim. Acta* **361**, 3903–3911 (2008)
10. E. Monzani, L. Casella, M. Gullotti, N. Panigada, F. Franceschi, V. Papaefthymiou, Cytochrome oxidase models. Dinuclear iron/copper complexes derived from covalently modified deuteroporphyrins. *J. Mol. Cat. A Chem.* **117**, 199–204 (1997)
11. T. Punniyamurthy, M.M. Reddy, S.J.S. Kalra, J. Iqbal, Cobalt(II) schiff base catalyzed biomimetic oxidation of organic substrates with dioxygen. *Pure Appl. Chem.* **68**, 619–622 (1996)

12. K.L. Nagashree, M.F. Ahmed, Electrocatalytic oxidation of methanol on Ni modified polyaniline electrode in alkaline medium. *J. Solid State Electrochem.* **14**, 2307–2320 (2010)
13. R.J.P. Williams, Metal ions in biological catalysts. *Pure Appl. Chem.* **54**, 1889–1904 (1982)
14. A. Deronzier, J.-C. Moutet, Functionalized polypyrroles. New molecular materials for electrocatalysis and related applications. *Acc. Chem. Res.* **22**, 249–255 (1989)
15. C.P. Horwitz, R.W. Murray, Oxidative electropolymerization of metal schiff base complexes. *Mol. Cryst. Liq. Cryst.* **160**, 389–404 (1988)
16. A. Ghaffari, M. Behzad, M. Pooyan, H.A. Rudbari, G. Bruno, Crystal structures and catalytic performance of three new methoxy substituted salen type nickel(II) Schiff base complexes derived from, meso-1,2-diphenyl-1,2-ethylenediamine. *J. Mol. Struct.* **2014**, 1–7 (1063)
17. Frank. Reuter, Eva. Rentschler, Structural, magnetic and electronic characterization of an isostructural series of dinuclear complexes of 3d metal ions bridged by tpbd. *Polyhedron* **52**, 788–796 (2013)
18. J.-C. Moutet, A. Ourari, Electrocatalytic epoxidation and oxidation with dioxygen using manganese(III) Schiff-base complexes. *Electrochim. Acta* **42**, 2525–2531 (1997)
19. J.-C. Moutet, Y. Ouennoughi, A. Ourari, S. H. -Thibault, Electrocatalytic hydrogenation on noble metal particles dispersed in polymer films. Enhanced catalytic activity induced by the incorporation of bimetallic catalysts. *Electrochim. Acta* **40**, 1827–1833 (1995)
20. B. Karlhuber, A. Fiaux, T. Schaffhauser, Ciba-Geigy Corporation, Process for producing epoxy resin having a low-EHC-content from chlorine-substituted crude epoxy resin of high EHC-content and apparatus for automatically controlling such process. Patent US4810776 (1989)
21. W. Zhang, J.L. Loebach, S.R. Wilson, E.N. Jacobsen, Enantioselective epoxidation of unfunctionalized olefins catalyzed by (Salen)manganese complexes. *J. Am. Chem. Soc.* **112**, 2801–2803 (1990)
22. R. Irie, K. Noda, Y. Ito, N. Matsumoto, T. Katsuki, Catalytic asymmetric epoxidation of unfunctionalized olefin. *Tetrahedron Lett.* **31**, 7345–7348 (1990)
23. A. Ourari, H. Nora, C. Noureddine, D. Aggoun, Elaboration of new electrodes with carbon paste containing polystyrene functionalized by pentadentate nickel(II)-Schiff base complex—application to the electrooxidation reaction of methanol and its aliphatic analogs. *Electrochim. Acta* **170**, 311–320 (2015)
24. A. Ourari, W. Derafa, D. Aggoun, A novel copper(II) complex with an unsymmetrical tridentate-schiff base: synthesis, crystal structure, electrochemical, morphological and electrocatalytic behaviors toward electroreduction of alkyl and aryl halides. *RSC Adv.* **5**, 82894–82905 (2015)
25. A. Ourari, Y. Ouennoughi, S. Bouacida, Tris(2-{[2-(4-methoxyphenyl)ethyl]imino methyl}phenolato-j2N,O1)cobalt(III), *Acta Cryst. E68, Struc. Reports m803–m804* (2012)
26. Y.-G. Li, D.-H. Shi, H.-L. Zhu, H. Yan, S.W. Ng, Transition metal complexes (M = Cu, Ni and Mn) of schiff-base ligands: syntheses, crystal structures, and inhibitory bioactivities against urease and xanthine oxidase. *Inorg. Chim. Acta* **360**, 2881–2889 (2007)
27. P. Singh, D.P. Singh, K. Tiwari, M. Mishra, A.K. Singh, V.P. Singh, Synthesis, structural investigations and corrosion inhibition studies on Mn(II), Co(II), Ni(II), Cu(II) and Zn(II) complexes with 2-amino-benzoic acid (phenyl-pyridin-2-yl-methylene)-hydrazide. *RSC Adv.* **5**, 45217–45230 (2015)
28. R. Aurkie, M.G. Rosair, R. Kadam, S. Mitra, Three new mono- di-trinuclear cobalt complexes of selectively and non-selectively condensed Schiff bases with N₂O and N₂O₂ donor sets: syntheses, structural variations. *EPR DNA Bind Stud Polyhedron* **28**, 796–806 (2009)
29. A. Ourari, K. Ouari, W. Moumeni, L. Sibous, G. Bouet, M.A. Khan, Unsymmetrical tetradentate schiff base complexes derived from 2,3-diaminophenol and salicylaldehyde or 5-bromosalicylaldehyde. *Trans. Met. Chem.* **31**, 169–175 (2006)
30. A.M.O. Ali, S.M. El-Medani, D.A. Ahmed, D.A. Nassar, Synthesis, characterization, fluorescence and catalytic activity of some new complexes of unsymmetrical Schiff base of 2-pyridinecarboxaldehyde with 2,6-diaminopyridine, *Spectrochim. Acta A Mol. Biomol. Spectrosc.* **144**, 99–106 (2015)
31. M. Mishra, K. Tiwari, A.K. Singh, V.P. Singh, Versatile coordination behavior of a multi-dentate Schiff base with manganese(II), copper(II) and zinc(II) ions and their corrosion inhibition study. *Inorg. Chim. Acta* **425**, 36–45 (2015)
32. S. Ilhan, H. Baykara, A. Oztomsuk, V. Okumus, A. Levent, M.S. Seyitoglu, S. Ozdemir, Synthesis and characterization of 1,2-bis(2-(5-bromo-2-hydroxybenzylideneamino)-4-chlorophenoxy)ethane and its metal complexes: an experimental, theoretical, electrochemical, antioxidant and antibacterial study, *Spectrochim. Acta A Mol. Biomol. Spectrosc.* **118**, 632–642 (2014)
33. M. Shebl, S.M.E. Khalil, S.A. Ahmed, H.A.A. Medien, Synthesis, spectroscopic characterization and antimicrobial activity of mono-, bi- and tri-nuclear metal complexes of a new Schiff base ligand. *J. Mol. Struct.* **980**, 39–50 (2010)

34. T. Rosu, E. Pahontu, C. Maxim, R. Georgescu, N. Stanica, A. Gulea, Some new Cu(II) complexes containing an ON donor Schiff base: synthesis, characterization and antibacterial activity. *Polyhedron* **30**, 154–162 (2011)
35. A.D. Khalaji, M. Nikookar, D. Das, Co(III), Ni(II), and Cu(II) complexes of bidentate N, O-donor Schiff base ligand derived from 4-methoxy-2-nitroaniline and salicylaldehyde Synthesis, characterization, thermal studies and use as new precursors for metal oxides nanoparticles. *J. Therm. Anal. Cal.* **115**, 409–417 (2014)
36. V.V. Sizov, M.V. Novozhilova, E.V. Alekseeva, M.P. Karushev, A.M. Timonov, S.N. Eliseeva, A.A. Vanin, V.V. Malev, O.V. Levin, Redox transformations in electroactive polymer films derived from complexes of nickel with SalEn-type ligands: computational, EQCM, and spectroelectrochemical study. *J. Solid State Electrochem.* **19**, 453–468 (2015)
37. A.H. Said, F.M. Mhalla, C. Amatore, J.-N. Verpeaux, Mechanistic investigation of the anodic oxidation of *p*-methoxytoluene in dry and wet acetonitrile. *J. Electroanal. Chem.* **464**, 85–92 (1999)
38. A.A. Isse, A. Gennaro, E. Vianello, Electrochemical reduction of Schiff base ligands H2salen and H2salophen. *Electrochim. Acta* **42**, 2065–2071 (1997)
39. S. Yagmur, S. Yilmaz, G. Saglikoglu, M. Sadikoglu, M. Yildiz, K. Polat, Synthesis, spectroscopic studies and electrochemical properties of Schiff bases derived from 2-hydroxy aromatic aldehydes and phenazopyridine hydrochloride. *J. Serb. Chem. Soc.* **78**(6), 795–804 (2013)
40. K. Aoki, K. Tokuda, H. Matsuda, Theory of linear sweep voltammetry with finite diffusion space: part II. Totally irreversible and quasi-reversible cases. *J. Electroanal. Chem.* **160**, 33–45 (1984)
41. K. Aoki, K. Tokuda, H. Matsuda, Theory of linear sweep voltammetry with finite diffusion space. *J. Electroanal. Chem.* **146**, 417–424 (1983)
42. A. Ourari, D. Aggoun, L. Ouahab, A novel copper(II)-Schiff base complex containing pyrrole ring: synthesis, characterization and its modified electrodes applied in oxidation of aliphatic alcohols. *Inorg. Chem. Commun.* **33**, 118–124 (2013)
43. A. Ourari, Y. Ouennoughi, D. Aggoun, M.S. Mubarak, E.M. Pasciak, D.G. Peters, Synthesis, characterization, and electrochemical study of a new tetradentate nickel(II)-Schiff base complex derived from ethylenediamine and 5'-(*N*-methyl-*N*-phenylaminomethyl)-2'-hydroxyacetophenone. *Polyhedron* **67**, 59–64 (2014)